ChemComm

COMMUNICATION

View Article Online
View Journal | View Issue

Cite this: *Chem. Commun.*, 2016, 52, 7683

Received 20th February 2016,
Accepted 17th May 2016

DOI: 10.1039/c6cc01558a

www.rsc.org/chemcomm

A photodegradable hexaaza-pentacene molecule for selective dispersion of large-diameter semiconducting carbon nanotubes†

Jie Han,‡[a] Qiyan Ji,‡[a] Hongbo Li,[a] Gang Li,[b] Song Qiu,*[a] Hai-Bei Li,*[b] Qichun Zhang,[c] Hehua Jin,[a] Qingwen Li*[a] and Jin Zhang[d]

Harvesting high-purity semiconducting single-walled carbon nanotubes (s-SWCNTs) with removable dispersants remains a challenge. In this work, we demonstrate that small heteroacene derivatives may serve as promising selective dispersants for sorting s-SWCNTs. A rich N "doped" and thiophene-substituted hexaazapentacene molecule, denoted as 4HP, was found to be more favorable for high-purity s-SWCNTs with large diameters. Importantly, 4HP is photodegradable under 365 nm or blue light, which enables a simple deposition approach for the formation of clean s-SWCNT networks. The as-fabricated thin film transistors show excellent performance with a charge-mobility of 30–80 $cm^2 V^{-1} s^{-1}$ and an on–off ratio of 10^4–10^6.

High-purity semiconducting single-walled carbon nanotubes (s-SWCNTs) become highly desirable for the fabrication of logic circuits, sensors and thin-film transistors due to their unique advantages in terms of mobility, flexibility, chemical stability and low-cost properties.[1] However, the co-existence of metallic and semiconducting SWCNTs in the as-produced raw materials makes the sorting of SWCNTs a great challenge.[2]

Designing conjugated polymers for the selective dispersion and enrichment of s-SWCNTs have gained intense interest recently, since the enriched s-SWCNT solution can be directly employed for the fabrication of thin-film transistors with greatly improved performance and processability.[3] Polyfluorene, polycarbazole, polythiophene and their copolymers have been extensively developed and it was demonstrated that their conjugated backbones and side chain structures are crucial for the wrapping and sorting of s-SWCNTs with good selectivity and dispersion in organic solvents.[4] Moreover, copolymer structures may lead to additional dispersion results. For example, left- and right-handed s-SWCNTs can be sorted when a copolymer is composed of fluorene with chiral binaphthol groups.[5] However, the limited species and the unmanageable batch differences coming from the polydispersity of the polymers will be the main challenge for the scale-up application of conjugated polymer-SWCNT hybrids. Meanwhile, polymer wrapping generally favors a complex spatial configuration leading to a difficulty in understanding the relationship between selectivity and the polymer structure clearly. As a result, designing the dispersant molecules with smaller size, better selectivity, and easier removability is a new target for further enhancing s-SWCNT based devices.

Herein, we report a small heteroacene derivative, which may serve as a promising selective dispersant for sorting s-SWCNTs. 2,3,9,10-Tetra-(5-hexyl-thiophen-2-yl)-1,4,6,8,11,13-hexaaza-pentacene, denoted as 4HP, was found to be more favorable for the high-yield extraction of high-purity s-SWCNTs with large diameters. Its rigid hexaaza-pentacene structure and two pairs of paw-like thiophene directed short alkyl chains more likely give rise to a unique selection effect on entrapping the s-SWCNTs with diameters >1 nm. Importantly, 4HP is photodegradable under 365 nm or blue light, which enables a simply deposition approach for the formation of clean s-SWCNT networks. The as-fabricated thin film transistors show excellent performance with a charge-mobility of 30–80 $cm^2 V^{-1} s^{-1}$ and an on–off ratio of 10^4–10^6.

Fig. 1a shows the molecular conformation of 4HP and the 4HP-SWCNT complex simulated using the PM6 semi-empirical *ab initio* method (PM6).[6] 4HP has good solubility in common organic solvents and can be easily synthesized through a one-step cyclocondensation reaction (Scheme S1, ESI†).[7] It can be seen that in a typical 4HP structure, a hexaazapentacene-based backbone is coupled with two pairs of paw-like thiophene directed alkyl chains. Due to the steric effect induced by two adjacent thiophene rings, the two pairs of short alkyl chains (C_6H_{12}) on both sides of 4HP are not in the same plane with its

[a] *Key Laboratory of Nanodevices and Applications, Suzhou Institute of Nanotech and Nanobionics, Chinese Academy of Science, Suzhou 215123, P. R. China. E-mail: sqiu2010@sinano.ac.cn, qwli2007@sinano.ac.cn*

[b] *School of Ocean, Shandong University, Weihai 264209, P. R. China. E-mail: lihaibei@sdu.edu.cn*

[c] *Division of Chemistry and Biological Chemistry, School of Physical and Mathematical Sciences, Nanyang Technological University, Singapore 63731, Singapore*

[d] *College of Chemistry and Molecular Engineering, Peking University, Beijing 100871, China*

† Electronic supplementary information (ESI) available. See DOI: 10.1039/c6cc01558a

‡ Jie Han and Qiyan Ji contributed equally to this work.

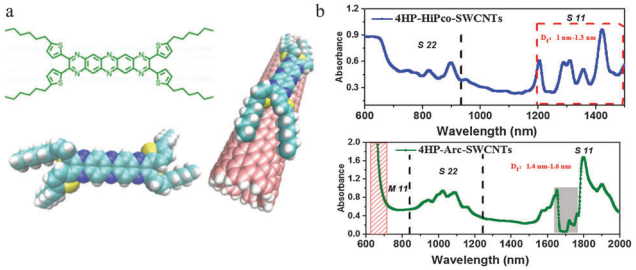

Fig. 1 (a) Chemical structure and conformation of a 4HP molecule and the complex of 4HP-SWCNT; (b) absorption spectra of 4HP-dispersed HiPco- and Arc-SWCNTs, in which the grey zone (1670–1770 nm) indicates the absorption of toluene.

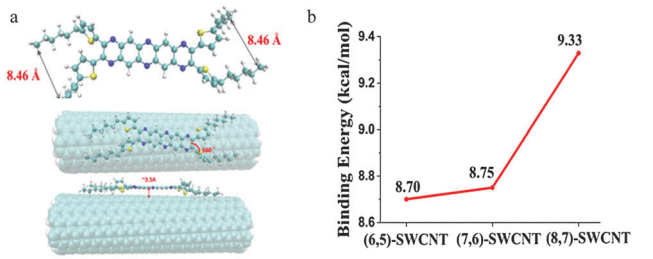

Fig. 2 (a) Structures obtained by the PM6 semi-empirical *ab initio* method: spatial conformation of an isolated 4HP molecule (top), structural variations for 4HP anchored on the s-SWCNTs with different chiralities (middle) and side view of the 4HP-s-SWCNT complex (bottom); (b) binding energies calculated for the 4HP-(*n*,*m*)-SWCNT complex.

hexaaza-pentacene-based backbone. As simulated, the high ratio of N heteroatoms in 4HP as well as its paw-like side-chains enables itself to uniquely anchor or clamp on a tube of desirable diameter, quite different from conventional planar aromatic polycyclic molecules, therefore presenting special structural discrimination for the s-SWCNTs upon dispersion.

Fig. 1b shows the typical absorption spectra of HiPco- and Arc-SWCNT solutions dispersed with 4HP in toluene. It can be clearly observed that 4HP exhibits unique selectivity on the large-diameter s-SWCNTs for the HiPco-nanotubes. Compared with the dispersions by most conjugated polymers in toluene reported so far, the 4HP induced HiPco-SWCNT dispersion showed a reduced number of absorption peaks from 600 nm to 1600 nm, with favorable bands distributed above 1200 nm, indicating that the s-SWCNTs were selectively enriched with diameters larger than 0.96 nm.[8] In order to further verify the unique selectivity of 4HP, Arc-SWCNTs with larger diameters (compared to HiPco-tubes) were tested. As expected, the resultant dispersion displayed a characteristic semiconducting excitation band at S22 (850–1200 nm) and suppressed at M11 (600–850 nm) corresponding to m-SWCNTs, confirming the availability of 4HP molecules in the selective extraction of large diameter s-SWCNTs and ignorance of the m-SWCNTs. However, the absorption between 600 nm and 700 nm is sharply increased with a tail in the M11 region, which would be caused by the strong absorption of 4HP in a far-visible regime (Fig. 5a). It's revealed that upon 4HP dispersion, the s-SWCNTs enriched from HiPco-tubes tend to distribute with diameters ranging from 0.96 nm to 1.32 nm, and the one from Arc-tubes tends to be larger than the HiPco-sample with diameters ranging from 1.38 nm to 1.61 nm, respectively.

Fig. 2 illustrates the possible interaction mode between 4HP and (*n*,*m*)-SWCNTs. We optimized all the structures of 4HP, (*n*,*m*)-SWCNT, and their complexes (4HP-SWCNT) using the semi-empirical PM6 method[6] implemented in Gaussian.[10] As seen from Fig. 2a, the isolated 4HP exhibits a rigid conjugated backbone composed of hexaaza-pentacene and relative flexible side chains. The distance between the two terminal carbon atoms of the adjacent alkyl chains is ~8.46 Å. The angle between the backbone and the side chain of the 4HP is around 160 degrees. It is worth noting that the structure of 4HP on the tube exhibits a significant variation compared with the isolated 4HP. According to simulation results, the distance between the two pairs of side chains becomes asymmetric and dependent on the SWCNT structures when anchored on the s-SWCNTs. For instance, the inter-chain distances at the two sides on (8,7)-SWCNT change to 4.02 Å and 8.00 Å respectively, shorter than that derived from the isolated 4HP (8.64 Å). While in the case of (6,5)-SWCNT, the inter-chain distances at the two sides adjust to 7.64 Å and 6.54 Å suggesting that the 4HP backbone tends to anchor on a tube in a preferable direction. Moreover, it's also revealed that the distance between the S-containing thiophene groups tend to approach closer to the tube surface than the N-containing hexaazapentacene backbone, probably indicating that the stronger interaction of the thiophene group with tubes ensures the paw-like alkyl chains to grab the SWCNTs tightly. Fig. 2b presents the binding energies of the 4HP molecules on the SWCNTs with different chiralities. The binding energy is the difference between the energy of the complex (4HP-(*n*,*m*)-SWCNT) and the sum of the isolated optimized monomers 4HP and (*n*,*m*)-SWCNT. We take (6,5)-SWCNT, (7,6)-SWCNT and (8,7)-SWCNT into consideration, which have a similar chirality but different diameters. It confirms well that the binding energy of 4HP on (*n*,*m*)-SWCNTs exhibits a rapid increase with the increase of the tubes' diameter.

Even though the length and position of the alkyl chain in conjugated polymers are the key factors to disperse and select s-SWCNTs,[3] small molecules may exhibit some unique properties in dispersing and sorting s-SWCNTs. There is no wonder that the most unique feature of 4HP is the higher ratio of heteroatoms than the reported conjugated molecules. In order to elucidate the important role of the heteroatoms (N and S) in 4HP in its unique dispersibility and selectivity for s-SWCNTs, XPS analysis was conducted to compare the binding energy of the heteroatoms with and without the dispersed s-SWCNTs. As shown in Fig. 3a, the typical N 1s peak was located at 400.2 eV for pure 4HP and shifted blue to 398.9 eV for 4HP dispersed s-SWCNTs. The energy difference between the nitrogen-atoms with and without s-SWCNTs can be as high as 1.3 eV, indicating a strong charge transfer interaction between the 4HP and the s-SWCNTs. Fig. 3b reveals that the typical high-resolution spectra of S 2p for pristine 4HP show two major peaks at around 165.4 and 166.6 eV with a spin-energy separation of 1.2 eV due to the presence of S=C bonds in the thiophene unit. When interacted with the s-SWCNTs, the two peaks exhibited 0.3 eV and 0.5 eV downshifts, respectively, more

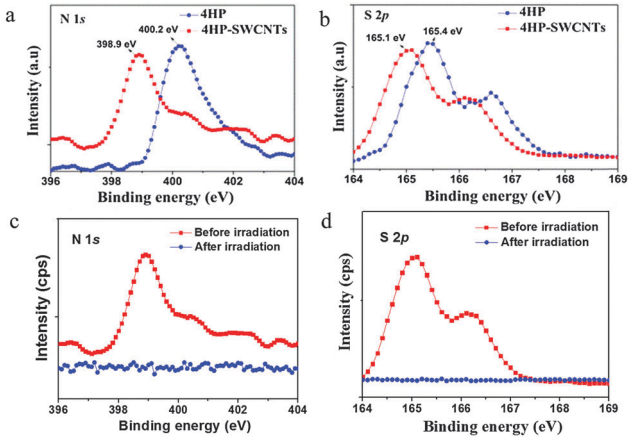

Fig. 3 XPS analysis on the possible interaction of 4HP with s-SWCNTs. (a and b) Binding energy variation of N 1s and S 2p peaks of 4HP before (blue line) and after (red line) interaction with SWCNTs; (c) and (d) XPS characterization for the 4HP-SWCNT complex (red line) and s-SWCNTs after irradiation under 365 nm light (blue line).

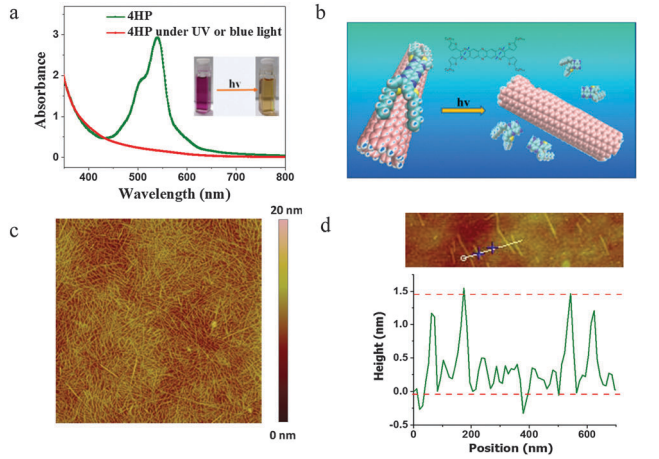

Fig. 4 (a) The spectroscopic change of 4HP solution during the photolysis by 365 nm or blue light; (b) the process of fabricating high-density and less dispersants thin films under UV or blue light; (c) the AFM image of 4HP-dispersed SWCNT networks between the two Au electrodes; (d) the diameter distribution of s-SWCNTs by a photodegradable process.

likely suggesting that the charge transfer also occurred between the thiophene units and the nanotubes. Comparatively, the stronger peak at around 165.4 eV for pristine 4HP downshifted to 163.92 eV for P3DDT and 164.32 eV for F8T2, respectively, correlating with different electronic states of S=C bonds among the three conjugated molecules.[3a,9] When wrapping s-SWCNTs, the peak slightly downshifted further for 0.2 eV for the P3DDT-SWCNTs and 0.1 eV for the F8T2-SWCNTs, respectively (shown in Fig. S3, ESI†). It supports the above hypothesis that the stronger interaction between the dispersant and the SWCNTs led to the better dispersibility of s-SWCNTs. On the other hand, it also reveals that the co-existence of N and S heteroatoms in the 4HP structure greatly enhances the interaction of 4HP with the s-SWCNTs, consequently leading to the high-yield sorting of s-SWCNTs. In order to detect whether the photolysis products had been removed from the tubes, XPS was conducted on the carbon nanotubes before and after irradiation with 365 nm or blue light. Fig. 3c and d compare the content variation of N and S elements on the surface of SWCNTs before and after 365 nm irradiation. The disappearance of N 1s and S 2p peaks indicate that 4HP or the photolysis production have been released from the surface of SWCNTs after undergoing a photolysis procedure.

Even though acidolysis has been tried to remove the polymers "shell", the second contamination by wet treatment may probably hamper its practical application.[11] Recently, it has been demonstrated that some delicate designed conjugated polymers could also be removed from the nanotubes and the clean-surface s-SWCNT film exhibited very good performance.[12] However, as a novel dispersant, it may contribute some exciting features. 4HP molecules are photodegradable, which may provide a promising method to remove or degrade the excessive dispersant molecules. After the filtration and washing process, the less-dispersant s-SWCNTs were redispersed in chloroform. Combining with the dip-coating method, we can obtain a high-density s-SWCNT film. This process confirmed that the deposited s-SWCNTs contained less dispersants. Fig. 4a shows the absorption spectra of 4HP in toluene before and after photo-degradation irradiation under 365 nm or blue light. The 4HP solution showed a broad absorption band from 450 nm to 700 nm. After irradiation under a laser beam at 365 nm or blue light with 10 watt power, the 4HP solution was faded into a light yellow solution in 15 minutes. Fig. 4b shows the photodegradable process of 4HP. When illuminated under 365 nm or blue light (435–450 nm) in solution, the backbone of 4HP is able to crack from the C=N bonds. Fig. 4c shows the morphology of the as-formed s-SWCNT network between the two Au electrodes. It's revealed that the s-SWCNTs in the network are still isolated with an average length around 1 μm. The AFM line profile showed height 1.4–1.5 nm, which indicate that the most 4HP clinging to the tubes were removed (Fig. 4d).

The obtained 4HP-s-SWCNT dispersion favors the fabrication of high-performance TFT devices. Pure 4HP showed poor charge mobility (<1 cm^2 V^{-1} s^{-1}). The photodegradable feature of 4HP confirms the fabrication of high-density and less dispersant films, which may be a promising method to fabricate high-performance thin-film devices. The as-dispersed network was used as the active layer, where the channel length and width for a TFT device were 20 μm and 200 μm, respectively. Fig. 5a and b displays the transfer and output curves for a typical device. A hole mobility of 65.2 cm^2 V^{-1} s^{-1} and an on–off ratio of 8×10^5 were obtained. In order to further verify the purity of s-SWCNTs, we fabricated the transistors with $L = 3$ μm and $W = 3000$ μm, which had an on–off ratio of 10^4 (Fig. S5, ESI†). Fig. 5c shows the on–off ratios of TFTs with different channel lengths and none of devices exhibited the on–off ratio lower than 10^4. Fig. 5d shows the histogram of mobilities of 25 TFTs and 60% devices have mobilities between 40 and 60 cm^2 V^{-1} s^{-1}. All of the devices showed excellent performance with the hole mobility scattering from 30–80 cm^2 V^{-1} s^{-1}. This also demonstrated 4HP to be an effective dispersant to induce

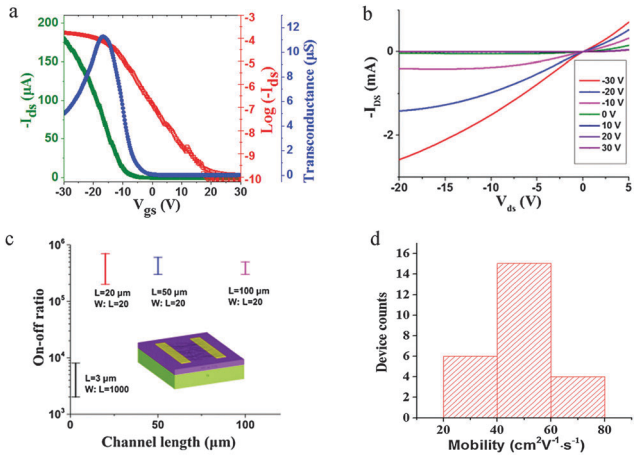

Fig. 5 (a and b) The transfer and output curves of a typical transistor (V_d = −1 V); (c) the on–off ratio of TFTs with a channel length ranging from 3 μm to 100 μm; (d) the histogram of the mobilities.

the high purity dispersion of large-diameter s-SWCNT solution. The paw-like entrapment and the special affinity of hexaaza-pentacene structures on the SWCNTs enable the unique selectivity and dispersibility of small 4HP molecules.

In conclusion, we have demonstrated that 4HP is able to show a unique preference for the selective entrapment of large diameter s-SWCNTs with high purity and yield. As aromatic hexaaza-pentacene derivatives are often photosensitive, the removal of excessive dispersant molecules can be readily achieved by photodegradation, meanwhile favoring the formation of surface-clean s-SWCNT networks. The as-fabricated TFT devices exhibited excellent performance with a charge-mobility of 30–80 $cm^2\ V^{-1}\ s^{-1}$ and an on–off ratio of 10^4–10^6, one of the best results reported so far. As a result, designing heteroatomic conjugated molecules with diverse structural backbones and specific spatial configuration may enrich our insights and strategies to manipulate the sorting of SWCNTs with different chiral structures and electronic properties.

The authors would like to thank Prof. M. Zheng for helpful discussion. This research was generously supported by the National Natural Science Foundation of China (No. 61274130, 21373262). H. B. acknowledges the Natural Science Foundation of Shandong Province, China (Grant No. ZR2014BQ015). Q. C. acknowledges the financial support AcRF Tier 1 (RG 16/12 and RG RG133/14) and Tier 2 (ARC 20/12 and ARC 2/13) from MOE, and CREATE program (Nanomaterials for Energy and Water Management) from NRF, Singapore.

Notes and references

1 (*a*) N. Rouhi, D. Jain and P. J. Burke, *ACS Nano*, 2011, **5**, 8471–8487; (*b*) S. Park, M. Vosguerichian and Z. Bao, *Nanoscale*, 2013, **5**, 1727–1752; (*c*) M. F. L. De Volder, K. S. H. Tawfic and R. H. Baughman, *Science*, 2013, **339**, 535–539.
2 M. C. Hersam, *Nat. Nanotechnol.*, 2008, **3**, 387–394.
3 (*a*) H. W. Lee, Y. Yoon, S. Park, J. H. Oh, S. Hong, L. S. Liyanage, H. Wang, S. Morishita, N. Patil, Y. J. Park, J. J. Park, A. Spakowitz, G. Galli, F. Gygi Wong, P. H.-S. Wong, J. B.-H. Tok, J. M. Kim and Z. Bao, *Nat. Commun.*, 2011, **2**, 1407–1422; (*b*) W. Gomulya, G. D. Costanzo, E. J. Figueiredo de Carvalho, S. U. Bisri, V. Derenskyi, M. Fritsch, N. Fröhlich, S. Allard, P. Gordiichuk, A. Herrmann, S. J. Marrink, M. C. Santos, U. Scherf and M. A. Loi, *Adv. Mater.*, 2013, **25**, 2948–2956; (*c*) H. Wang, J. Mei, P. Liu, K. Schmidt, G. Jiménez-Osés, S. Osuna, L. Fang, C. J. Tassone, A. P. Zoombelt, A. N. Sokolov, K. N. Houk, M. F. Toney and Z. Bao, *ACS Nano*, 2013, **7**, 2659–2668.
4 (*a*) S. K. Samanta, M. Fritsch, U. Scherf, W. Gomulya, S. Z. Bisri and M. A. Loi, *Acc. Chem. Res.*, 2014, **47**, 2446–2456; (*b*) K. S. Mistry, B. A. Larsen and J. L. Blackburn, *ACS Nano*, 2013, **7**, 2231–2239; (*c*) F. Chen, Toward the Extraction of Single Species of Single-Walled Carbon Nanotubes Using Fluorene-Based Polymers, *Nano Lett.*, 2007, **7**, 3013–3017.
5 K. Akazaki, F. Toshimitsu, H. Ozawa, T. Fujigaya and N. Nakashima, *J. Am. Chem. Soc.*, 2012, **134**, 12700–12707.
6 J. J. Stewart, *J. Mol. Model.*, 2007, **13**, 1173–1213.
7 G. Li, J. Gao and Q. Zhang, *Asian J. Org. Chem.*, 2014, **3**, 203–208.
8 R. B. Weisman and S. M. Bachilo, *Nano Lett.*, 2003, **3**, 1235–1238.
9 Z. Liu, H. Li, Z. J. Qiu, S. L. Zhang and Z. B. Zhang, *Adv. Mater.*, 2012, **24**, 3633–3638.
10 S. Bourgoin-Voillard, E. L. Zins, F. Fournier, Y. Jacquot, C. Afonso, C. Pepe, G. Leclercq and J. C. Tabet, *J. Am. Soc. Mass Spectrom.*, 2009, **20**, 2318–2333.
11 F. Toshimitsu and N. Nakashima, *Nat. Commun.*, 2014, **5**, 5041.
12 (*a*) T. Lei, X. Chen, G. Pitner, H.-S. P. Wong and Z. Bao, *J. Am. Chem. Soc.*, 2016, **138**, 802–805; (*b*) I. Pochorovski, H. Wang, J. Feldblyum, X. Zhang, A. Antaris and Z. Bao, *J. Am. Chem. Soc.*, 2015, **137**, 4328–4331.

